Fish and Shellfish Immunology 88 (2019) 627–635

Contents lists available at ScienceDirect

Fish and Shellfish Immunology

journal homepage: www.elsevier.com/locate/fsi

Full length article

Characterisation and function of *TRIM23* in grass carp (*Ctenopharyngodon idella*)

Pengfei Chu[a,b], Libo He[a], Cheng Yang[a,b], Yangyu Li[a,b], Rong Huang[a], Lanjie Liao[a], Yongming Li[a], Zuoyan Zhu[a], Yaping Wang[a,*]

[a] State Key Laboratory of Freshwater Ecology and Biotechnology, Institute of Hydrobiology, Chinese Academy of Sciences, Wuhan, 430072, China
[b] University of Chinese Academy of Sciences, Beijing, 100049, China

ARTICLE INFO

Keywords:
TRIM23
Grass carp (*Ctenopharyngodon idella*)
Innate immune
Subcellular localisation
BIFC
Autophagy

ABSTRACT

Tripartite motif (TRIM) proteins are key components of the innate immune system, functioning as antiviral restriction factors or modulating signaling cascades that lead to proinflammatory cytokine induction. In the present study, the TRIM family gene *TRIM23* from grass carp (*Ctenopharyngodon idella*) was cloned and characterised. *TRIM23* was moderately expressed in the examined tissues, and the significantly altered expression was observed after grass carp reovirus (GCRV) and poly(I:C) infection. Dual-luciferase activity assay showed that TRIM23, especially its C-terminal domain ARF, depressed the promoter activity of *IRF3* and *IRF7*. The subcellular localisation showed that TRIM23 protein was located in the cytoplasm and could be recruited by both TRAF6 and MyD88. Furthermore, TRIM23 was confirmed to interact with either TRAF6 or MyD88 by the bimolecular fluorescence complementation (BiFC) system in CIK cells. Additionally, autophagy was enhanced by over-expressed TRIM23 in 293T cells. Taken together, our results demonstrate that *TRIM23* gene plays an important role in innate immune regulation and provide new insights into understanding the functional characteristics of the *TRIM23* in teleosts.

1. Introduction

Innate immune responses are activated by the engagement of pattern recognition receptors (PRRs) recognizing the invaded pathogen [1–3]. Subsequently, various immune responses were initiated, including the production of cytokines and the initiation of pro-inflammatory and adaptive immune responses [4]. The tripartite motif-containing (TRIM) superfamily (also known as RBBC superfamily) contains about 100 members in humans and most of them have emerged as key components of the innate immune system, functioning as antiviral restriction factors or involving in a broad range of biological processes that are associated with innate immunity [5–9].

TRIM proteins belong to the larger family of RING E3 ligases and most of the numbers compose a Really Interesting New Gene (RING) zinc finger domain, one or two B-box domains and an associated coiled-coil domain in the amino-terminal region [5]. The RING domain is a specialised type of zinc finger that is located in the N-terminal portion of almost all TRIM proteins and confers E3 ligase activity by binding to an ubiquitin-loaded E2 enzyme and promoting the transfer of ubiquitin to a target protein [5,7,10,and11]. Recently, many TRIM family members have been confirmed to mediate ubiquitylation events depending on the RING domain. The RING-finger-type E3 ubiquitin ligase of TRIM5α could ubiquitinate itself in cooperation with the E2 ubiquitin-conjugating enzyme UbcH5B [12]. Activator-recruited cofactor 105-kDa component (ARC105)-mediated transcriptional activation induced by transforming growth factor β (TGFβ) signaling is regulated by TRIM11 through an ubiquitin-mediated degradation pathway [13]. The RING domain of TRIM21 facilitates and enhances the polyubiquitination chains of mitochondrial antiviral-signaling protein (MAVS) [14,15]. The catalytic amino acids Cys15 and Cys18 of the RING domain are required for TRIM22 antiviral activity [16]. TRIM25 involves in not only for RIG-I ubiquitination but also for RIG-I-mediated interferon-β production and antiviral activity in response to RNA virus infection [17]. The B-box domains flanked RING domain have different consensus sequences between members of the TRIM superfamily [4]. Interestingly, some evidences have showed that B-box domains may contribute to innate resistance to HIV. Studies on HIV showed that B-box 2 of TRIM5α influences the recognition of the viral capsid by the carboxy-terminal PRYSPRY domain and the ability of TRIM15 to mediate HIV restriction [18,19]. B-Box C-terminal domain (BBC) is always a coiled-coil domain which mediates homomeric and heteromeric interactions among TRIM family members and other proteins, in

* Corresponding author.
E-mail address: wangyp@ihb.ac.cn (Y. Wang).

https://doi.org/10.1016/j.fsi.2019.03.025
Received 13 December 2018; Received in revised form 12 March 2019; Accepted 12 March 2019
Available online 16 March 2019

particular self-association [4]. The C terminus of TRIM family members contain various domains among different species. The contribution of these domains to the regulation of innate immune responses has yet to be well established.

The number of TRIMs varies greatly in different species. More than 100 members encoded by the humans genome excluding pseudogenes, 208 trim genes in the zebrafish (*Danio rerio*) and 66 in pufferfish (*Tetraodon nigroviridis*) were identified by whole genome sequencing [9,20,21and22], thus demonstrating their ancient separation from each species [23]. Recent studies showed that a large family numbers of TRIMs play a significant role in fish immunity [9]. TRIM14, 51, 67, 72, 82, 83 and 99 in grass carp were identified by bioinformatics analysis [23], however, little TRIMs functional information of regulation in innate immune was reported. In the study, the TRIM family gene *TRIM23* in grass carp (*Ctenopharyngodon idella*) was cloned and characterised. Expression profiles in different tissues and in response to GCRV and poly(I:C) infection were examined. In *C. idella* kidney (CIK) cells, the regulation of promoter activity of *IRF3* and *IRF7* by TRIM23 was analysed. Additionally, the subcellular localisation of TRIM23 protein and the interaction with TRAF6 and MyD88 were visualized. Furthermore, the enhanced autophagy in 293T cells transfected with pCMV-HA-TRIM23 was explored. These findings will provide new insights for understanding the functions of *TRIM23* gene in teleosts.

2. Materials and methods

2.1. Experimental fish and cells

Six-month-old grass carps (weight, 40 ± 10 g; length, 15 ± 3 cm) used in the study were provided by the GuanQiao Experimental Station, Institute of Hydrobiology, Chinese Academic of Sciences, and acclimatized in aerated freshwater at 28 °C. The fish were fed twice a day with a commercial feed (Tong Wei, China). Grass carps were acclimatized for 1 week and used for the following experiments after no abnormal symptoms were observed. The CIK cells (China Center for Type Culture Collection, China) used in the study were maintained in low glucose Dulbecco's modified Eagle's medium (DMEM; Hyclone, USA) supplemented with 10% fetal bovine serum at 28 °C in a humidified atmosphere with 5% CO_2 and 1% (v/v) penicillin-streptomycin. The 293T cells were a kind gift from Professor Wei Hu, Institute of Hydrobiology, Chinese Academy of Sciences.

2.2. Cloning the full-length cDNA of TRIM23

The matched fragments of *TRIM23* were obtained by blasting the homologous *TRIM23* sequences (Accession no. NM_001076644) of zebrafish (*Danio rerio*) with draft genome of grass carp [24]. 5′ and 3′ untranslated regions (UTRs) of the *TRIM23* gene were obtained by the rapid amplification of cDNA ends (RACE) PCR according to 5′ and 3′ Full RACE Kit (TaKaRa, Japan). The coding sequences (CDS) were amplified using PCR with primers within the 5′- and 3′-UTRs. The PCR products were purified, ligated into pMD18-T vectors (TaKaRa, Japan), and transformed into competent *Escherichia coli* DH5α cells (TransGen, China). Ten positive colonies were selected and sequenced by a commercial company (Tsing Ke, China). The full-length cDNA of *TRIM23* were obtained by comparing these PCR product sequences and discarding the obtained overlapping region sequences and vector sequences. The primers used for gene cloning and sequence verification were listed in Table S1.

2.3. Sequence analysis

BLAST (https://blast.ncbi.nlm.nih.gov/Blast.cgi) was used to search for gene and protein sequences in other species. Amino acid sequences of TRIM23 proteins were predicted using open reading frame (ORF) Finder (http://www.ncbi.nlm.nih.gov/projects/gorf/), and multiple sequence alignments were performed using ClustalW 2.1 (http://www.ebi.ac.uk/tools/clustalw2.1). SMART (http://smart.embl-heidelberg.de/) was used to predict the protein domain features. Neighbour-joining (NJ) phylogenetic trees were constructed on the basis of the amino acid sequences by using MEGA 7.0 software (http://www.megasoftware.net/index.html) and the bootstrap values of the branches were obtained by testing the tree 1000 times.

2.4. GCRV challenge and sampling

The GCRV preparation and GCRV challenge experiment were carried out as described previously [25]. Six uninfected fish were selected as the control group before the GCRV challenge experiment was conducted, and samples of the middle kidney, head kidney, liver, intestine, spleen, and gill were collected. Afterward, the tissues were also randomly sampled from six infected fish for six consecutive days after intraperitoneal injection. All samples were homogenized in TRIzol reagent (Invitrogen, USA) and stored at −80 °C prior to RNA extraction.

2.5. Tissue distribution of TRIM23 in grass carp

The total RNA was extracted from the tissues and then reverse-transcribed to obtain cDNA as described previously [26]. In order to explore the tissue distribution of *TRIM23* in healthy grass carp, qRT-PCR and the CFX96™ real-time PCR detection system (Bio-Rad, USA) were used to measure the mRNA expression levels of *TRIM23*. The housekeeping gene *β-actin* was used as a reference gene. Relative expression levels were calculated as the ratio of gene expression in each tissue relative to that in the head kidney. The specific primers for qRT-PCR were listed in Table S1. Relative expression levels of *TRIM23* were calculated using the $2^{-\triangle\triangle Ct}$ method [27].

2.6. Responses of TRIM23 to GCRV infection

Firstly, the dynamic changes of GCRV in infected grass carps were determined, the relative copy number of the viruses in the intestine and gill on day 1, 3, and 5 were examined by RT-qPCR using specific primers (Table S1) for the S6 segments of GCRV-II. For convenience, the relative copy number of GCRV on day 1 after infection were used as a reference for normalization.

In addition, the mRNA expression levels of *TRIM23* in the middle kidney, head kidney, liver, and spleen of six grass carp at different days after GCRV infection (1, 2, 3, 4, 5, and 6 days) were used to examine the responses of *TRIM23* to GCRV infection. The *β-actin* gene was used as a reference gene. Relative expression levels were calculated as the ratio of gene expression in the infected grass carps at each time point (1, 2, 3, 4, 5, and 6 days after GCRV infection) relative to that in the uninfected fish (0 day). The specific primers for qRT-PCR were listed in Table S1.

2.7. Construction of plasmid vectors

To analyse the role of *TRIM23* in *IFN-I* signal pathway, plasmid pCMV-HA-TRIM23, pGL3-IRF3, and pGL3-IRF7 were constructed. The restriction sites *EcoR*I and *Kpn*I (NEB, USA) were introduced to construct pCMV-HA-TRIM23 as described previously [28]. Briefly, plasmid pCMV-HA (Clontech, USA) was linearized with *EcoR*I and *Kpn*I, products were recovered by gel cutting and purification. Secondly, *TRIM23* ORF from grass carp was amplified by specific primer which was designed by CE Design (http://www.vazyme.com). Lastly, linearized pCMV-HA together with *TRIM23* ORF was incubated at 37 °C for 30 min and then incubated on the ice straightway, according to the manufacturer's instructions of ClonExpress kit (Vazyme, USA). Except for pCMV-HA-TRIM23, recombinant plasmids contained different TRIM23 protein domains including pCMV-HA-TRIM23 (aa96-594), (aa1-406), (aa1-95), (aa407-594) were also constructed (primers were listed in Table S1). Plasmids pGL3-IRF3 and pGL3-IRF7 were constructed as following

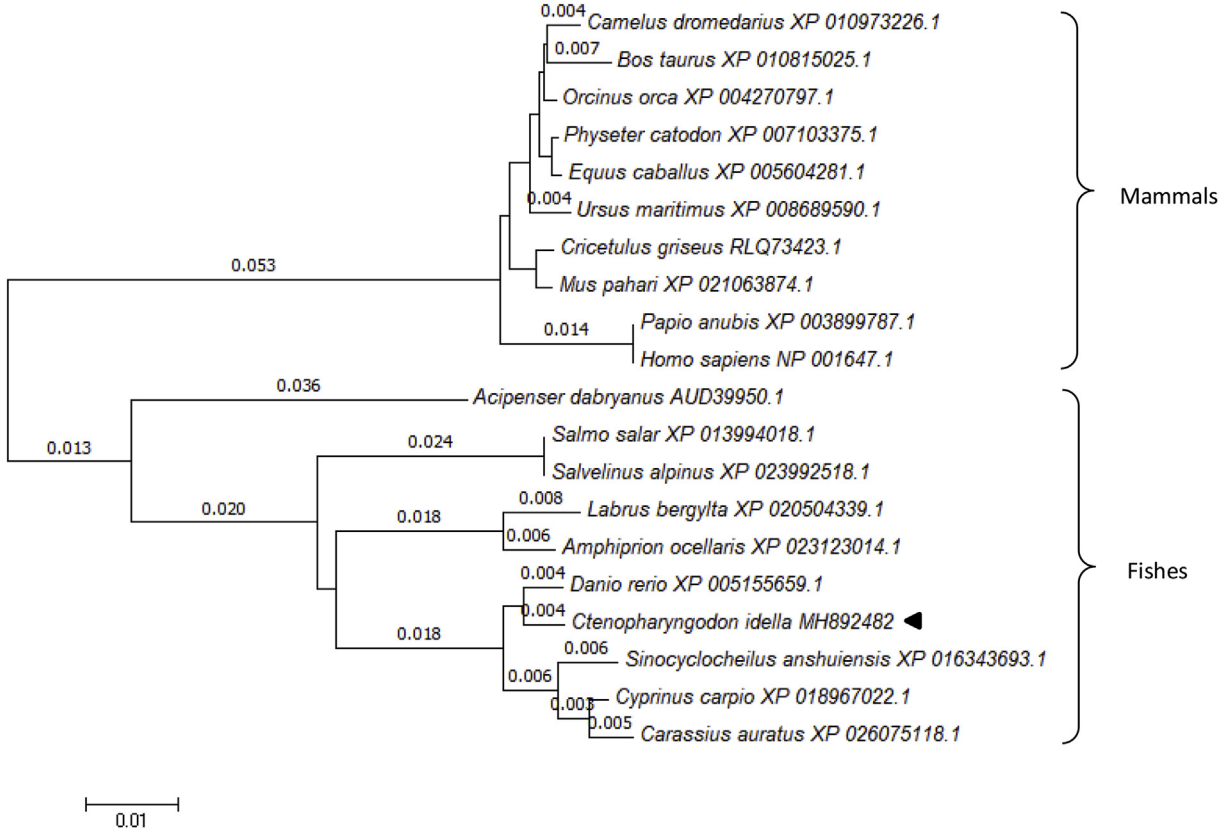

Fig. 1. Neighbour-joining phylogenetic tree analysis of TRIM23. The tree was constructed based on amino acid sequences of grass carp TRIM23 and 19 orthologs using MEGA 7.0 software and the bootstrap values of the branches were obtained by testing the tree 1000 times.

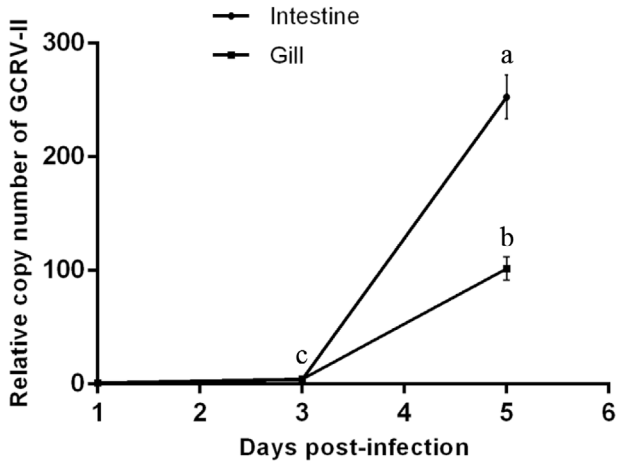

Fig. 2. Relative copy number of GCRV-II in infected grass carp. The relative copy number of GCRV-II were examined by using specific primers in S6 segment. The copy number of GCRV-II on day 1 after infection were used as a reference for normalization. Error bars indicate standard deviation. The data (expressed as mean ± standard deviation) were analysed by one-way analysis of variance, followed by Dunnett's test for multiple comparisons using SPSS Statistics 19 software. Different days labelled with different letters indicate statistically significant differences in mRNA levels ($p < 0.05$).

method. Digestion with *Kpn*I and *Xho*I and ligation with T4 DNA Ligase, the promoter region of *IRF3* and *IRF7* were cloned, digested and subcloned into *Kpn*I and *Xho*I sites of pGL3-Basic luciferase reporter vector (Promega, USA) (primers were listed in Table S2).

In order to further understand the functions of TRIM23 protein, TRIM23-pDsRed vector was constructed as the same method described above. The restriction sites *Eco*RI and *BamH*I (NEB, USA) were introduced and subcloned into the same digested restriction sites of pDsRed2-C1 vector (Clontech, USA) to construct pDsRed-TRIM23. Recombinant plasmids of TRAF6-pEGFP and MyD88-pEGFP were constructed previously [28] and kept in the lab. Besides, pTRIM23-MN155, pMC156-TRAF6, and pMC156-MyD88 were constructed to analyse the interaction of TRIM23 with TRAF6 and MyD88 proteins. Briefly, the ORF sequences of TRIM23, TRAF6, and MyD88 (introduced with the restriction sites *Hind*III and *Kpn*I) were cloned from grass carp and inserted into the pMN155 or pMC156 plasmids, respectively (The plasmids pMN155 and pMC156 used in the study were a kind gift from Professor Zongqiang Cui, Wuhan Institute of Virology, Chinese Academy of Sciences and kept in our lab). The final recombinant plasmids were named pTRIM23-MN155, which contained the N-terminal of mNeptune (mNeptune aa 1–155, MN155), pMC156-TRAF6, and pMC156-MyD88, which contained the C-terminal of mNeptune (mNeptune aa 156C-terminal, MC156), respectively (primers were listed in Table S2). All the sequences of the resulting plasmids were verified by DNA sequencing.

2.8. Responses of TRIM23 in CIK cells after poly(I:C) stimulation

CIK cells seeded in six-well plates were stimulated with poly(I:C) (sigma, USA) at a final concentration of 20 μg/ml or phosphate-buffered saline (PBS) as control groups. Cells from each group were harvested at 3, 8, 24, 36, and 48 h after poly(I:C) stimulation and total RNA was extracted and reverse transcribed to cDNA. Then the cDNA was used as a template for qRT-PCR to determine the expression levels of *TRIM23*.

2.9. Dual-luciferase activity assays

CIK were seeded in each well of 12-well plate and incubated at 28 °C overnight. Subsequently, the cells were transfected with 500 ng of

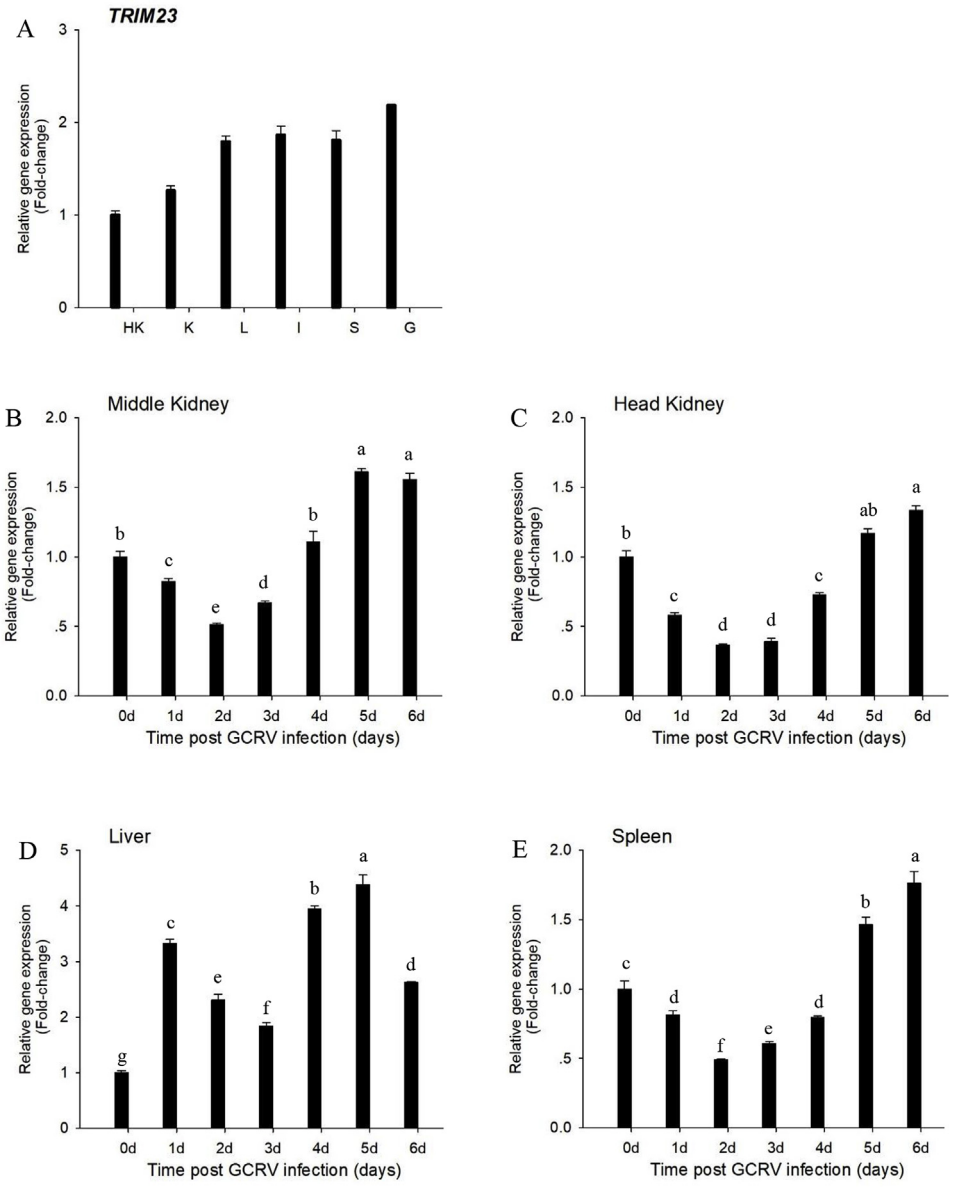

Fig. 3. Tissue distribution of *TRIM23* and expression pattern following GCRV infection. RNA was isolated from the middle kidney (K), head kidney (HK), liver (L), intestine (I), spleen (S), and gill (G) and subjected to qRT-PCR analysis. A. Relative expression levels of *TRIM23* were calculated on the basis of the ratio of gene expression in the different tissues relative to that in the head kidney. The expression levels of *β-actin* were used as an internal control. B-E. Expression levels of *TRIM23* in the healthy group (day 0) were set to 1 and *β-actin* was used as an internal control to normalize the relative expression levels of *TRIM23* in different tissue following GCRV infection. Error bars indicate standard deviation. The data (expressed as mean ± standard deviation) were analysed by one-way analysis of variance, followed by Dunnett's test for multiple comparisons using SPSS Statistics 19 software. Different days labelled with different letters indicate statistically significant differences in mRNA levels ($p < 0.05$).

pGL3-IRF3, or pGL3-IRF7, 500 ng of pCMV-HA-TRIM23 or pCMV-HA-TRIM23 (aa96-594), (aa1-406), (aa1-95), (aa407-594) or empty vector, and 10 ng of pRL-TK Renilla plasmid (Promega, USA) for 6 h. Then the medium was renewed by DMEM supplemented with 10% FBS and 1% penicillin-streptomycin for 24h. Cells were lysed by 300 ml of 1 × Passive Lysis Buffer (Promega, USA) and luciferase activities were measured by using a Dual-Luciferase Reporter Assay System (Promega, USA).

2.10. Subcellular localisation of TRIM23 and related proteins

To analyse the subcellular localisation of TRIM23, TRIM23-pDsRed vector was constructed. The day before transfection, CIK cells were plated evenly in six-well plates with glass bottom for 24 h to 70–80% confluence. Then, the vectors were transiently transfected into the CIK cells as the method described above. To further investigate the relationship between TRIM23 and related proteins, TRIM23-pDsRed was transfected into CIK cells together with TRAF6-pEGFP or MyD88-pEGFP vectors, respectively as described above. After 24 h transfection, all cells were fixed with 4% paraformaldehyde, and stained with Hoechst 33342 (Beyotime, China). The CIK cells were observed using the UltraVIEW VOX confocal system (PerkinElmer, Fremont, CA, USA) and a 63× oil immersion objective lens.

2.11. Validation of the interaction between TRIM23 and related proteins

The bimolecular fluorescence complementation (BiFC) system was introduced to detect whether TRIM23 could interact with TRAF6 and MyD88. Plasmids pTRIM23-MN155, which contained the N-terminal of mNeptune (mNeptune aa 1–155, MN155) alone or together with pMC156-TRAF6 or pMC156-MyD88, which contained the C-terminal of mNeptune (mNeptune aa 156C-terminal, MC156) were transfected into CIK cells as described above. After 24 h transfection, the cells were fixed with 4% paraformaldehyde, and stained with Hoechst 33342 (Beyotime, China). The CIK cells were observed using the UltraVIEW VOX confocal system (PerkinElmer, Fremont, CA, USA) and a 63× oil immersion objective lens.

2.12. The function of TRIM23 in autophagy

To assess the role of TRIM23 protein in autophagy, 293T cells were plated evenly in six-well plates with glass bottom for 16 h to 70–80%

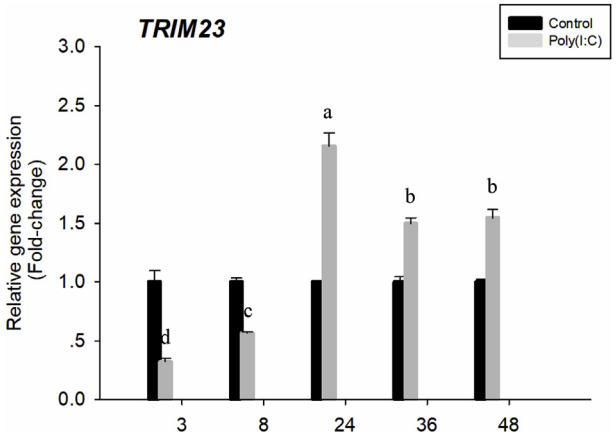

Fig. 4. Analysis of *TRIM23* gene expression after poly(I:C) stimulation. RNA was isolated from each cells group (3, 8, 24, 36, and 48 h after poly (I:C) stimulation) subjected to qRT-PCR analysis. Expression levels of *TRIM23* gene in the PBS group at each point were set to 1 and *β-actin* was used as an internal control to normalize the relative expression levels of *TRIM23*. Error bars indicate standard deviation. The data (expressed as mean ± standard deviation) were analysed by one-way analysis of variance, followed by Dunnett's test for multiple comparisons using SPSS Statistics 19 software. Different hours labelled with different letters indicate statistically significant differences in mRNA levels ($p < 0.05$).

confluence. Then, TRIM23-pDsRed or pDsRed-C1 vector were transiently transfected into the 293T cells as the method described above. After 12 h transfection, the cells were incubated with Ad-GFP-LC3B (Beyotime, China), which could express the hallmark of autophagy induction, a green fluorescent protein (GFP)-LC3B puncta [29]. After 36 h incubation, the cells were fixed with 4% paraformaldehyde and stained with Hoechst 33342 (Beyotime, China). The 293T cells were observed using the UltraVIEW VOX confocal system (PerkinElmer, Fremont, CA, USA) and a 63× oil immersion objective lens.

2.13. Statistical analysis

The statistical results (expressed as mean ± standard deviation) were analysed by one-way analysis of variance, followed by Dunnett's test for multiple comparisons using SPSS Statistics 19 software. $p < 0.05$ was considered to be statistically significant. All experiments were repeated at least three times.

3. Results

3.1. Molecular characterisation and phylogenetic analysis of TRIM23

The full length cDNA of *TRIM23* (Genbank accession number: MH892482) is 2390 bp long, with a 1785 bp ORF encoding a predicted polypeptide of 594 amino acids, 72 bp 5′ UTR, and 533 bp 3′ UTR (Fig. S1). Structure analysis revealed that TRIM23 consisted of two conserved BBOX (aa 142–188, aa 193–239) flanked by an N-terminal

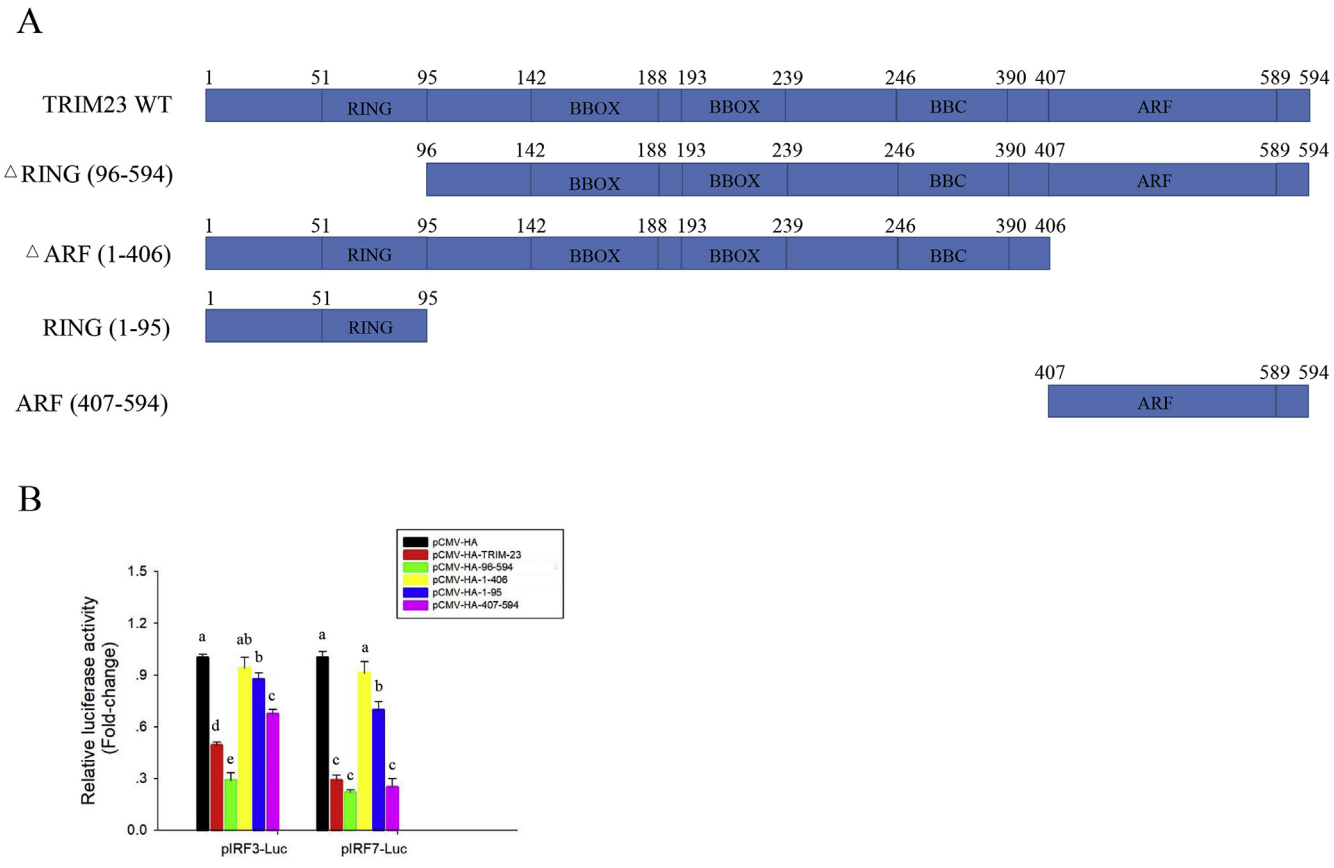

Fig. 5. The regulation of *TRIM23* on the promoter activity of *IRF3* and *IRF7*. A. Schematic diagram of recombinant plasmids contained the domain organization of TRIM23 with approximate residue boundaries. B. The promoter activity of *IRF3* and *IRF7* is monitored by dual-luciferase activity assays in CIK cells co-transfected with pCMV-HA-TRIM23 (or pCMV-HA-TRIM23 (aa96-594), (aa1-406), (aa1-95), (aa407-594), or empty vector) and pGL3-IRF3, or pGL3-IRF7 and pRL-TK Renilla plasmid. Renilla luciferase activity was examined as the internal control and relative luciferase activity levels were expressed as fold increase of luciferase activity. Error bars indicate standard deviation. The data (expressed as mean ± standard deviation) were analysed by one-way analysis of variance, followed by Dunnett's test for multiple comparisons using SPSS Statistics 19 software. Different domains labelled with different letters indicate statistically significant differences in luciferase activity ($p < 0.05$).

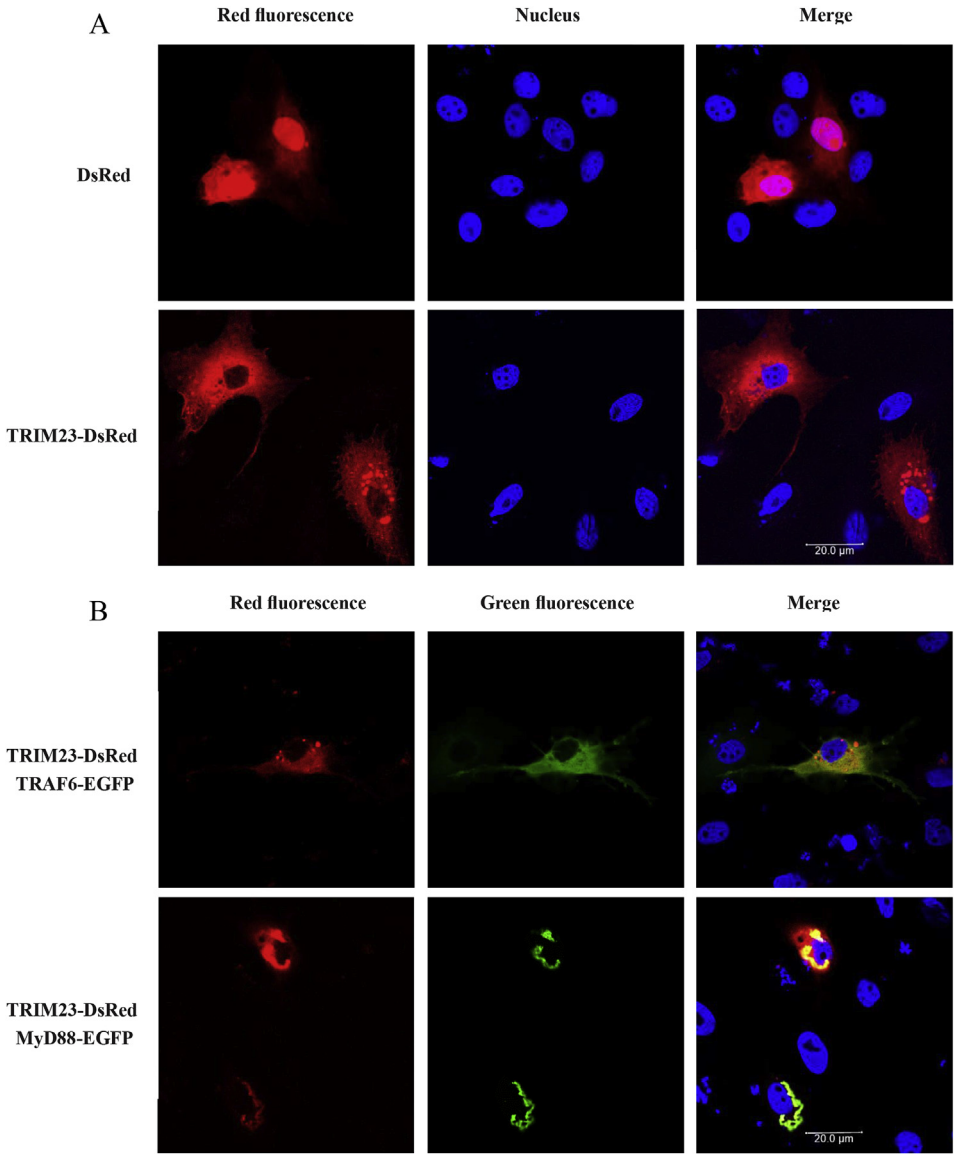

Fig. 6. Subcellular localisation of TRIM23, TRAF6, and MyD88 in CIK cells. Cells were transfected with the plasmids TRIM23-pDsRed alone or co-transfected with TRAF6-pEGFP or MyD88-pEGFP, and fluorescence was observed at 24 h after transfection. Red/Green fluorescence showed the distribution of pDsRed/EGFP-tagged proteins, and blue fluorescence showed the nucleus stained with Hoechst 33342 under a 63× oil immersion objective lens (scale bar, 20 μm).

conserved Ring finger domain (RING, aa 51–95), and a B-Box C-terminal domain (BBC, aa 246–390) in the middle, followed by a C-terminal domain of ADP-ribosylation factor (ARF) (aa 407–589). Evolutionary relationship analysis based on the full-length amino acid sequences of TRIM23 with other species revealed that TRIM23 could be classified into two groups: TRIM23 proteins from the fishes fell into one branch; TRIM23 proteins from mammals fell into another branch. TRIM23 from grass carp was closely related to that of *D.rerio*. (Fig. 1).

3.2. Relative copy number of the GCRV in grass carp

To determine the dynamic changes of GCRV in infected grass carps, the relative copy number of the viruses on day 1, 3, and 5 were examined by RT-qPCR using specific primers for the S6 segments of GCRV-II. For convenience, the relative copy number of GCRV on day 1 after infection were used as a reference for normalization. As shown in Fig. 2, the relative copy number of GCRV were consistent or increased slightly in first three days both in the intestine and gill after infection, while a marked increase emerged on day 5 after infection. Furthermore, the relative copy number of GCRV in the intestine were about 2.5 times as many as that in the gill on day 5 after infection.

3.3. Tissue distribution of TRIM23 in healthy grass carp

Six tissue samples (middle kidney (K), head kidney (HK), liver (L), intestine (I), spleen (S), and gills (G)) were isolated from healthy grass carps for qRT-PCR to analyse the tissue distribution of the *TRIM23* gene in grass carp. As shown in Fig. 3, *TRIM23* was mainly enriched in the gill and expressed the lowest in the head kidney.

3.4. Analysis of TRIM23 expression following GCRV infection

To determine whether *TRIM23* is involved in the innate immune responses to GCRV infection, the relative mRNA expression levels of *TRIM23* on different days after infection were examined by RT-qPCR. As shown in Fig. 3, following GCRV stimulation, *TRIM23* mRNA expression levels were altered in all the detected tissues. In the middle kidney, head kidney, and spleen, *TRIM23* were downregulated on the first two days after GCRV infection, then, increased steadily and reached the peak on the day 6 (in the head kidney and spleen) or day 5

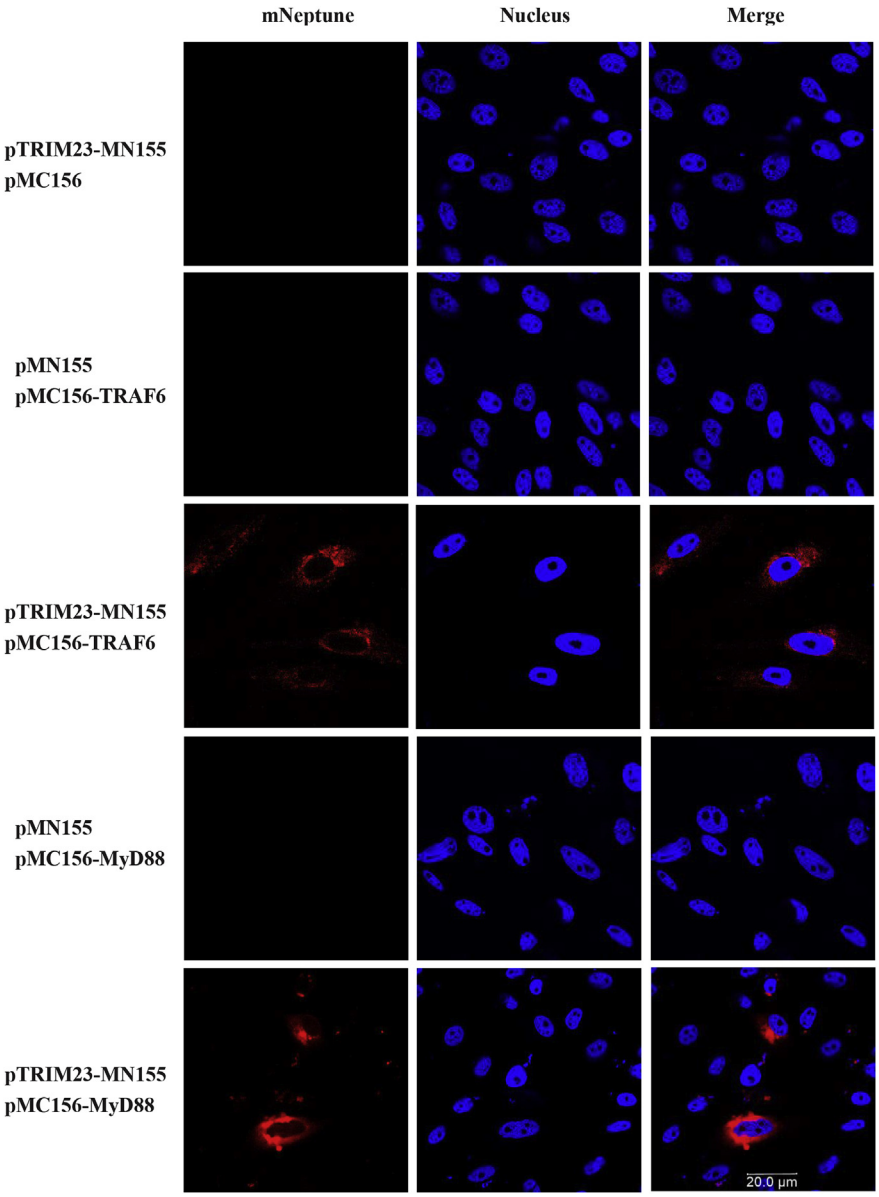

Fig. 7. The interaction of TRIM23 with TRAF6 and MyD88. Imaging of the protein-protein interaction was visualized by using far-red mNeptune-based BiFC in *vivo*. Plasmids pTRIM23-MN155 and pMC156-TRAF6 or pMC156-MyD88 were co-transfected into CIK cells together. In the BiFC system, the fluorescence of the mNeptune channel was red, and the nucleus was stained with Hoechst 33342. The images were acquired using fluorescence microscopy and a 63× oil immersion objective lens (scale bar, 20 μm).

(in the middle kidney). In the liver, *TRIM23* mRNA expression levels were up-regulated significantly on day 1, subsequently, slightly down-regulated in next two days, then sharply up-regulated again and peaked on day 5, afterward decreased at the late stage.

3.5. Analysis of TRIM23 expression following poly(I:C) stimulation in CIK cells

In order to explore the functions of *TRIM23* during innate immune, the mRNA expression levels of *TRIM23* were detected after poly(I:C) stimulation in CIK cells. As shown in Fig. 4, compared to the control, the expression levels of *TRIM23* were significantly decreased at 0h–8h after poly(I:C) stimulation, subsequently, dramatically up-regulated and reached the peak at 24h following poly(I:C) stimulation, afterward it decreased at the late stage.

3.6. TRIM23 depressed the promoter activity of IRF3 and IRF7

To analyse the role of grass carp *TRIM23* in *IRF-I* signal pathway, further experiments were performed to assess the effect of *TRIM23* on the transcriptional regulation of the promoter in *vivo*. The plasmids pCMV-HA-TRIM23 or others structural domain of TRIM23 plasmids were co-transfected into CIK cells with pGL3-IRF3, or pGL3-IRF7 and pRL-TK Renilla plasmid. As shown in Fig. 5, compared to the control, TRIM23 significantly depressed the promoter activity of *IRF3* and *IRF7*, besides, the C-terminal domain ARF exerted a more powerful ability than other domain regions to depress the promoter activity of *IRF3* and *IRF7*.

3.7. Subcellular localisation of TRIM23 and related proteins

To investigate the subcellular localisation of the TRIM23 protein, CIK cells were transfected with TRIM23-pDsRed plasmids, and then

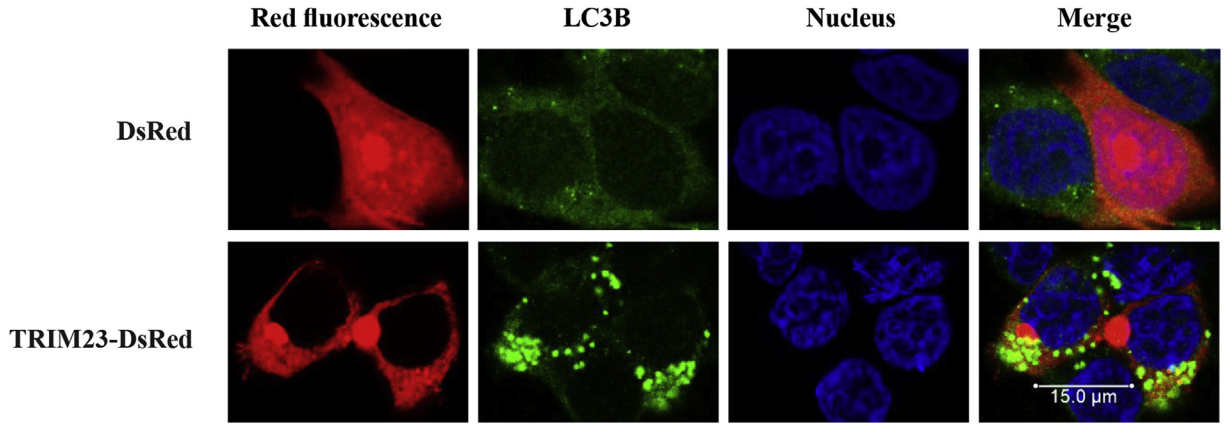

Fig. 8. TRIM23 promoted autophagy. 293T cells had been transfected with TRIM23-pDsRed for 12 h, then cells were incubated with Ad-GFP-LC3B. After 36 h incubation, the cells were fixed with 4% paraformaldehyde and stained with Hoechst 33342. The images were acquired using fluorescence microscopy and a 63× oil immersion objective lens (scale bar, 15 μm).

fluorescence was observed at 24 h after transfection. The empty pDsRed2-C1 plasmids were also transfected at the same time and used as the negative control. As shown in Fig. 6, the control pDsRed2-C1 was strongly distributed uniformly throughout the entire cell, while TRIM23-pDsRed was only strongly distributed in the cytoplasm.

Further, the relationship between TRIM23 and related proteins was also investigated. TRIM23-pDsRed were transfected into CIK cells together with TRAF6-pEGFP or MyD88-pEGFP, respectively. As shown in Fig. 6, co-localisation was observed between TRAF6/MyD88 and TRIM23, especial for MyD88, thus suggesting that TRAF6 and MyD88 could recruit and relocate TRIM23 protein.

3.8. TRIM23 could interact with TRAF6 and MyD88

In the study, the mNeptune-based BiFC system was used to visualize the interaction of TRAF6 and MyD88 with TRIM23 in CIK cells. As shown in Fig. 7, CIK cells co-transfection with pTRIM23-MN155 and pMC156-TRAF6 or pMC156-MyD88 resulted in a bright red mNeptune fluorescence signal in the cytoplasm surrounding the cell nucleus. However, the bright red mNeptune fluorescence signal was not observed when it came to the co-transfection with pTRIM23-MN155 and pMC156, or pMN155 and pMC156-TRAF6, or pMN155 and pMC156-MyD88. Thus, the results further confirmed that TRIM23 could interact with both TRAF6 and MyD88 in CIK cells.

3.9. TRIM23 promoted autophagy

To corroborate the role of TRIM23 in autophagy, 293T cells were used to overexpress TRIM23 protein. The green fluorescent protein (GFP)-LC3B puncta in 293T cells could show the hallmark of autophagy induction. As shown in Fig. 8, compared to the control, TRIM23 proteins detectably induced GFP-LC3B puncta formation in the cytoplasm. Besides, the place where GFP-LC3B puncta occurred was also coincident with the subcellular localisation of TRIM23 protein described previously.

4. Discussion

TRIM family proteins are critical E3 ligase family in many cellular functions, including the regulation and coordination of innate immunity and antiviral responses [30–34]. In recent years, a great number of studies have been focused on their regulatory role in innate immunity and the pathogenesis of many diseases [35]. In the study, dramatic changes of *TRIM23* expression levels after GCRV infection predicted that TRIM23 may be involved in grass carp hemorrhagic disease (Fig. 3). In order to explore the function of TRIM23, The full length cDNA of *TRIM23* was cloned and the protein sequences were predicted. Phylogenetic tree analysis showed that TRIM23 protein of grass carp was closely related to that of zebrafish (Fig. 1), just like other reported family numbers [23]. TRIM proteins are such named due to their conserved domain [36]. Like human TRIMs, the TRIM23 protein of grass carp also has conserved domain, including a RING zinc finger domain in the N-terminal, two B-box, a B-Box C-terminal domain in the middle and a C-terminal domain of ARF (Fig. 5). The RING domain of TRIMs was well known as mediating the interaction with ubiquitin-bound E2 via the zinc finger motifs [37–39]. A few role on the B-box were characterised including its coordinating TRIM self-association and protein–protein interactions [39]. The B-Box C-terminal domain was always a hyper-helical structure and usually considered to allow for dimerization and self-association [40,41]. The variable C-terminal region of TRIMs expand the diversity and functionality of this protein family, to date, 11 classes of TRIM C-terminal domains have been characterised [39]. The C-terminal region of grass carp TRIM23 is ARF. In order to explore the role of grass carp *TRIM23* in the transcriptional regulation of *IFN-I* signal pathway, eukaryotic expression plasmid pCMV-HA-TRIM23 and other plasmids containing different domain region were constructed. Luciferase activity analysis showed that the CIK cells transfected with pCMV-HA-TRIM23 exerted repressed promoter activity of *IRF3* and *IRF7*, compared to the cell transfected with empty vector. In addition, the ARF C-terminal domain exerted a more powerful ability than other domain regions to suppress the promoter activity of *IRF3* and *IRF7*.

The expression pattern analysis of grass carp indicated constitutive expression of *TRIM23* mRNA in various tissues. It is interesting that *TRIM23* mRNA expression levels were significantly decreased in the middle kidney, head kidney, and liver at the early state of GCRV infection, and this pattern of expression was consistent with that in poly (I:C)-infected CIK cells (Figs. 3 and 4). Previous study showed that *IFN-I* mRNA expression levels in the middle kidney, head kidney, and liver of grass carp were all up-regulated at the early state of poly(I:C) infection [42]. We guess this may be closely related with the role of *TRIM23* in the transcriptional regulation of *IFN-I* signal pathway.

Increasing evidences indicates that TRIMs can act as antiviral factors indirectly by stimulating cytokine signaling pathways [4, 32, 34, and 43]]. It has been reported that TRIM23 ubiquitinates the ubiquitinbinding protein NEMO for IRF3 and NF-κB activation. In addition, the interaction between TRAF3 and TRIM23 were observed in coimmunoprecipitation assays. However, how TRAF3 transmits antiviral signals to the TRIM23-NEMO complex remain unknown [44]. In the study, the interaction of TRIM23 with TRAF6 and MyD88 was visualized by subcellular localisation and BIFC system (Figs. 6 and 7). The subcellular localisation of TRIM23 protein in the cytoplasm was also

consistent with previous data (Fig. 6) [45]. However, how TRIM23 transmits signals to downstream signaling cascades by interaction with TRAF6 and MyD88 should be examined in the future. Furthermore, autophagy has been increasingly appreciated as an important mechanism in antimicrobial defences [46–48]. The induced autophagy experiment was also performed in 293T cells in the study, interestingly, 293T cells transfected with pDsRed-TRIM23 resulted into a greater extent of autophagy induction than did the cells transfected with empty vector (Fig. 8) [44], which indicated the diverse roles of TRIM23.

In conclusion, the characterisation and transcriptional regulation pattern of *TRIM23* from grass carp were described and discussed. TRIM23 involvement in the transcriptional regulation of to *IRF3* and *IRF7*, as well as its role in autophagy, strengthens the hypothesis that TRIM23 evolvd as a component of the innate immune regulation. Furthermore, the interaction of TRIM23 with TRAF6 and MyD88 may provide new insights into understanding the functional characteristics of the *TRIM23* in teleosts.

Acknowledgments

This work was funded by the National Natural Science Foundation of China [grant number 31572614], the Strategic Pilot Science and Technology Projects (A) Category, Chinese Anatomical Society [grant number XDA08030203], the State Key Laboratory of Freshwater Ecology and Biotechnology [grant number 2016FBZ02], the National Natural Science Foundation of China [grant number 31702332], and the Hubei Natural Science Foundation of China [grant number 2017CFB374].

Appendix A. Supplementary data

Supplementary data to this article can be found online at https://doi.org/10.1016/j.fsi.2019.03.025.

References

[1] L.A. O'Neill, A.G. Bowie, The family of five: TIR-domain-containing adaptors in Toll-like receptor signaling, Nat. Rev. Immunol. 7 (5) (2007) 353–364.
[2] S. Akira, S. Uematsu, O. Takeuchi, Pathogen recognition and innate immunity, Cell 124 (4) (2006) 783–801.
[3] T. Kawai, S. Akira, Innate immune recognition of viral infection, Nat. Immunol. 7 (2006) 131–137.
[4] K. Ozato, D.M. Shin, T.H. Chang, et al., TRIM family proteins and their emerging roles in innate immunity, Nat. Rev. Immunol. 8 (11) (2008) 849–860.
[5] A. Reymond, G. Meroni, A. Fantozzi, et al., The tripartite motif family identifies cell compartments, EMBO J. 20 (9) (2014) 2140–2151.
[6] R. Rajsbaum, J.P. Stoye, A. O'Garra, Type I interferon-dependent and -independent expression of tripartite motif proteins in immune cells, Eur. J. Immunol. 38 (3) (2010) 619–630.
[7] L.J. Crawford, C.K. Johnston, A.E. Irvine, TRIM proteins in blood cancers, J. Cell Commun. Signal. 12 (1) (2018) 21–29.
[8] A. Borlepawar, N. Frey, A.Y. Rangrez, A systematic view on E3 ligase Ring TRIMmers with a focus on cardiac function and disease, Trends Cardiovasc. Med. (2018), https://doi.org/10.1016/j.tcm.2018.05.007.
[9] T. Kimura, A. Jain, S.W. Choi, et al., TRIM-directed selective autophagy regulates immune activation, Autophagy 13 (5) (2017) 989–990.
[10] M. Torok, L.D. Etkin, Two B or not two B? Overview of the rapidly expanding B-box family of proteins, Differentiation 67 (3) (2010) 63–71.
[11] E. Toniato, X. Chen, J. Losman, et al., TRIM8/GERP RING finger protein interacts with SOCS-1, J. Biol. Chem. 277 (40) (2002) 37315–37322.
[12] K. Yamauchi, K. Wada, K. Tanji, et al., Ubiquitination of E3 ubiquitin ligase TRIM5α and its potential role, FEBS J. 275 (7) (2010) 1540–1555.
[13] H. Ishikawa, H. Tachikawa, Y. Miura, et al., TRIM11 binds to and destabilizes a key component of the activator-mediated cofactor complex (ARC105) through the ubiquitin-proteasome system, FEBS Lett. 580 (20) (2006) 4784–4792.
[14] B. Xue, H. Li, M. Guo, et al., TRIM21 promotes innate immune response to RNA viral infection through lys27-linked polyubiquitination of MAVS, J. Virol. (2018), https://doi.org/10.1128/JVI.00321–18.
[15] A. Sabile, A.M. Meyer, C. Wirbelauer, et al., Regulation of p27 degradation and S-phase progression by Ro52 RING finger protein, Mol. Cell Biol. 26 (16) (2006) 5994–6004.
[16] S.D. Barr, J.R. Smiley, F.D. Bushman, The interferon response inhibits HIV particle production by induction of TRIM22, PLoS Pathog. 4 (2) (2008) e1000007.
[17] C.H. Joo, TRIM25 RING-finger E3 ubiquitin ligase is essential for RIG-I-mediated antiviral activity, Nature 446 (7138) (2007) 916–920.
[18] D.M. Dykxhoorn, Y. Benita, N. Yan, et al., Identification of host proteins required for HIV infection through a functional genomic screen, Science 319 (5865) (2008) 921–926.
[19] X. Li, B. Song, Sh.H. Xiang, JosephSodroski, Functional interplay between the B-box 2 and the B30.2(SPRY) domains of TRIM5α, Virology 366 (2) (2007) 234–244.
[20] D.M. Dawidziak, J.G. Sanchez, J.M. Wagner, et al., Structure and catalytic activation of the TRIM23 RING E3 ubiquitin ligase, Proteins Struct. Funct. Bioinf. 85 (10) (2017) 1957–1961.
[21] L.M. Van Der Aa, J.P. Levraud, M. Yahmi, et al., A large new subset of TRIM genes highly diversified by duplication and positive selection in teleost fish, BMC Biol. 7 (1) (2009) 1–23.
[22] P. Boudinot, L.M. Van Der Aa, L. Jouneau, et al., Origin and evolution of TRIM proteins: new insights from the complete TRIM repertoire of zebrafish and pufferfish, PLoS One 6 (7) (2011) e22022.
[23] K. Luo, Y.Sh. Li, K.T. Ai, et al., Bioinformatics and expression analysis of finTRIM genes in grass carp, *Ctenopharyngodon idella*, Fish Shellfish Immunol. 66 (2017) 217–223.
[24] Y. Wang, Y. Lu, Y. Zhang, et al., The draft genome of the grass carp (*Ctenopharyngodon idellus*) provides insights into its evolution and vegetarian adaptation, Nat. Genet. 47 (6) (2015) 625–631.
[25] P. Chu, L. He, L. Xiong, et al., Molecular cloning, expression analysis and localization pattern of the MST family in grass carp (*Ctenopharyngodon idella*), Fish Shellfish Immunol. 76 (2018) 316–323.
[26] P. Chu, L. He, Y. Li, et al., Molecular cloning and functional characterisation of *NLRX1* in grass carp (*Ctenopharyngodon idella*), Fish Shellfish Immunol. 81 (2018) 276–283.
[27] K.J. Livak, T.D. Schmittgen, Analysis of relative gene expression data using realtime quantitative PCR and the $2^{-\triangle\triangle Ct}$ method, Methods 25 (4) (2001) 402–408.
[28] P. Chu, L. He, D. Zhu, et al., Identification, characterisation and preliminary functional analysis of *IRAK-M* in grass carp (*Ctenopharyngodon idella*), Fish Shellfish Immunol. 84 (2019) 312–321.
[29] K.M.J. Sparrer, S. Gableske, M.A. Zurenski, et al., TRIM23 mediates virus-induced autophagy via activation of TBK1, Nat. Microbiol. 2 (2017) 1543–1557.
[30] R. Rajsbaum, A. Garcia-Sastre, G.A. Versteeg, Trimmunity: the roles of the TRIM E3-ubiquitin ligase family in innate antiviral immunity, J. Mol. Biol. 426 (2014) 1265–1284.
[31] G.A. Versteeg, S. Benke, A. Garcia-Sastre, et al., Intrimsic immunity: positive and negative regulation of immune signaling by tripartite motif proteins, Cytokine Growth Factor Rev. 25 (2014) 563–576.
[32] P.D. Uchil, A. Hinz, S. Siegel, et al., TRIM protein-mediated regulation of inflammatory and innate immune signaling and its association with antiretroviral activity, J. Virol. 87 (2013) 257–272.
[33] P.D. Uchil, B.D. Quinlan, W.T. Chan, et al., TRIM E3 ligases interfere with early and late stages of the retroviral life cycle, PLoS Pathog. 4 (2008) e16.
[34] G.A. Versteeg, R. Rajsbaum, M.T. Sanchez-Aparicio, et al., The E3-ligase trim family of proteins regulates signaling pathways triggered by innate immune pattern-recognition receptors, Immunity 38 (2013) 384–398.
[35] J. Lascano, P.D. Uchil, W. Mothes, et al., TRIM5 retroviral restriction activity correlates with the ability to induce innate immune signaling, J. Virol. 90 (1) (2016) 308–316.
[36] S. van Tol, A. Hage, M.I. Giraldo, et al., TRIMendous role of TRIMs in virus–host interactions, Vaccines (Basel). 5 (3) (2017) 23.
[37] P. Ebner, G.A. Versteeg, F. Ikeda, Ubiquitin enzymes in the regulation of immune responses, Crit. Rev. Biochem. Mol. Biol. 52 (4) (2017) 425–460.
[38] Y. Ye, M. Rape, Building ubiquitin chains: E2 enzymes at work, Nat. Rev. Mol. Cell Biol. 10 (2009) 755–764.
[39] D. Esposito, M.G. Koliopoulos, K. Rittinger, Structural determinants of TRIM protein function, Biochem. Soc. Trans. 45 (2017) 183–191.
[40] M.G. Koliopoulos, D. Esposito, E. Christodoulou, et al., Functional role of TRIM E3 ligase oligomerization and regulation of catalytic activity, EMBO J. 35 (2016) 1204–1218.
[41] J.G. Sanchez, K. Okreglicka, V. Chandrasekaran, et al., The tripartite motif coiled-coil is an elongated antiparallel hairpin dimer, Proc. Natl. Acad. Sci. U.S.A. 111 (2014) 2494–2499.
[42] D. Li, W. Tan, M. Ma, et al., Molecular characterization and transcription regulation analysis of type I IFN gene in grass carp (*Ctenopharyngodon idella*), Gene 504 (1) (2012) 31–40.
[43] T. Kawai, S. Akira, Regulation of innate immune signaling pathways by the tripartite motif (TRIM) family proteins, EMBO Mol. Med. 3 (2011) 513–527.
[44] Kei-i. Arimoto, K. Funami, Y. Saeki, et al., Polyubiquitin conjugation to NEMO by triparite motif protein 23 (TRIM23) is critical in antiviral defense, Proc. Natl. Acad. Sci. Unit. States Am. (2010), https://doi.org/10.1073/pnas.1004621107.
[45] A. Reymond, G. Meroni, A. Fantozzi, et al., The tripartite motif family identifies cell compartments, EMBO J. 20 (2001) 2140–2151.
[46] M.C. Tal, A. Iwasaki, Autophagy and innate recognition systems, Curr. Top. Microbiol. Immunol. 335 (2009) 107–121.
[47] B. Levine, N. Mizushima, H.W. Virgin, Autophagy in immunity and inflammation, Nature 469 (2011) 323–335.
[48] V. Deretic, T. Saitoh, S. Akira, Autophagy in infection, infammation andimmunity, Nat. Rev. Immunol. 13 (2013) 722–737.